An R package for atmospheric thermodynamics

Jon Sáenz[a,b,*], Santos J. González-Rojí[a], Sheila Carreno-Madinabeitia[c,a],
Gabriel Ibarra-Berastegi[d,b]

[a]*Dept. Applied Physics II, Universidad del País Vasco-Euskal Herriko Unibertsitatea (UPV/EHU), Barrio Sarriena s/n, 48940-Leioa, Spain.*
[b]*BEGIK Joint Unit IEO-UPV/EHU, Plentziako Itsas Estazioa (PIE, UPV/EHU), Areatza Pasealekua, 48620 Plentzia, Spain*
[c]*Meteorology Area, Energy and Environment Division, TECNALIA R&I, Basque Country, Spain.*
[d]*Dept. Nuc. Eng. and Fluid Mech., Universidad del País Vasco-Euskal Herriko Unibertsitatea (UPV/EHU), Alameda Urquijo s/n, 48013-Bilbao, Spain.*

Abstract

This is a non-peer reviewed preprint submitted to EarthArxiv. It is the authors' version initially submitted to Computers and Geosciences corresponding to final paper "Analysis of atmospheric thermodynamics using the R package aiRthermo", published in Computers and Goesciences after substantial changes during the review process with doi: `http://doi.org/10.1016/j.cageo.2018.10.007`, which the readers are encouraged to cite.

In this paper the publicly available R package *aiRthermo* is presented. It allows the user to process information relative to atmospheric thermodynamics that range from calculating the density of dry or moist air and converting between moisture indices to processing a full sounding, obtaining quantities such as Convective Available Potential Energy, additional instability indices or adiabatic evolutions of particles. It also provides the possibility to present the information using customizable Stüve diagrams. Many of the functions are written inside a C extension so that the computations are fast. The results of an application to five years of real soundings over the Iberian Peninsula are also shown as an example. Thus, the package considerably extends the capabilities in R for the processing of atmospheric soundings or model results. This will hopefully have impact in many practical applications of environmental forecasting at different scales such as statistical downscaling for climate analysis, quantitative precipitation forecast (particularly precipitation extremes), the diagnosis of storms, flash floods, lightning, aviation and other fields where the computation of quantities related to atmospheric convection is important.

---

*Corresponding author: Jon Sáenz
Email addresses: `jon.saenz@ehu.eus` (Jon Sáenz), `santosjose.gonzalez@ehu.eus` (Santos J. González-Rojí), `sheila.carreno@tecnalia.com` (Sheila Carreno-Madinabeitia), `gabriel.ibarra@ehu.eus` (Gabriel Ibarra-Berastegi)
URL: `http://www.ehu.eus/eolo` (Jon Sáenz)

Authorship statement: Jon Sáenz had the original concept of the package, wrote most parts of the C code, several parts of the R code and some of the verification routines. He was also the lead author of the paper. Santos J. González-Rojí wrote some parts of the R and verification codes, packaged the software for its inclusion in CRAN and wrote some parts of the paper. Sheila Carreno-Madinabeitia was the author of the Stüve plotting routines and

Declarations of interest:

The only interest of the authors is to make the package known. If the paper is accepted, their scientific merit will also be publicly recognized.

Highlights

1. A new package providing new functionalities in the field of atmospheric thermodynamics to the R programming language is presented.
2. The most critical functions are written in C to speed up computations.
3. It provides numerical results and Stüve diagrams not previously available in R.
4. A realistic application has been produced for a case-study covering five years of twice-daily soundings over the Iberian Peninsula (2010-2014).
5. The package can be a key part of advanced forecast systems and diagnostics for extreme events (floods, storms, ...).

1. Introduction

R (`https://www.cran.r-project.org/`) is a freely available software for statistical computing that in the last years has grown exponentially. One of the key aspects to explain its success is its structure, consisting of a core module and more than 12000 libraries or packages specifically developed for different purposes. The number of available libraries increases literally every day with new developments. Thus, many research communities in different fields are increasingly adopting R as a tool for data analysis.

Some packages in the intersection between air pollution, climate and atmospheric studies make R a powerful tool for data processing and visualization of atmospheric processes such as air pollution [1], hydrology [2], mapping [3], the processing of satellite [4] and atmospheric data [5]. Additional useful packages in this field such as RAtmosphere, ClimDown, opentraj and others can be downloaded from the CRAN repository.

However, the analysis of atmospheric soundings or water vapour in the atmosphere from the perspective of atmospheric thermodynamics are still areas where the authors identified new needs for the community of atmospheric scientists using R. *aiRthermo* extends the functionality offered by packages `RadioSonde` and `meteogRam` by adding Stüve diagrams and vertical evolution of air parcels.

Under the conditions of pressure and temperature found in the atmosphere, the state of dry air is commonly described by two thermodynamic variables (such as pressure P and temperature T). The concentration of water can be expressed by means of different moisture indices such as specific humidity, mixing ratio, virtual temperature and relative humidity. Phase changes of water produce large latent heat fluxes that must be considered as air parcels ascend or descend [6, 7, 8] during the study of atmospheric stability and convection.

Some indices of instability are often used in the diagnostics of meteorological situations. For example: the relationship between sea breeze and precipitation over Hainan Island [9], the role of moist convection in the development of flash floods [10] or the retrieval of precipitation in the TRMM mission [11] to name a few. Thermodynamical variables and indices are also used for statistical downscaling of extreme precipitation events and moisture transports [12].

The main objective of this paper is to present an R package designed to allow scientists to perform computations involving atmospheric thermodynamics from inside the R language. This considerably extends the capabilities of R for meteorological data analysis. This has allowed us, for instance, to extend the lectures offered at the M. Sc. level [13] enabling students to perform numerical exercises related with these quantities.

2. Data

2.1. Sample data provided with the package

The data used in Section 4 of this paper (provided in the package for easy testing by users) were collected from the server located at the University of Wyoming. The first sounding used in this paper (sounding A) corresponds to Santander, Spain, (station ID 08023, date 2010-06-16, 12:00 UTC). It corresponds to a day that produced some frontal rain. The second case (sounding D) corresponds to Barcelona, Spain, (station ID 08190, 2013-08-07, 12:00 UTC)
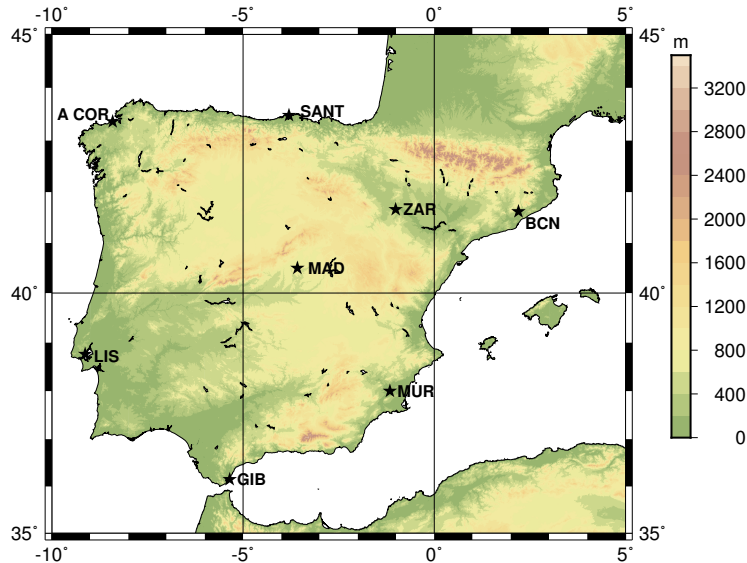
Figure 1: Map of the Iberian Peninsula with the stations where soundings are routinely made.

and reflects a situation with substantial convective instability. The last example (Davenport, USA, station ID 74455, 1997-06-21 at 00 UTC) is also used to illustrate a case with strong convection [14].

2.2. Data for the case study

The topography of the Iberian Peninsula and the position of the eight sounding sites over it are shown in Figure 1. The sounding files downloaded from Wyoming University's server covered the period 2010-2014. The number of cases depends on the site and range from 1705 over Lisbon to 3575 over Murcia. The values of instability indices as computed at Wyoming University and by using the functions in *aiRthermo* were compared. In *aiRthermo*, initial conditions for CAPE were obtained by vertically averaging the lowest 500 m of the sounding and performing isobaric precooling of the resulting low-level average particle.

3. Methodology

Most of the theory and methods used in *aiRthermo* can be found in standard references [6, 7, 8, 15, 14]. However, some of the assumptions made are documented below.

The state of an air parcel is defined in *aiRthermo* by means of its pressure P (Pa), temperature T (K) and mixing ratio w (kg kg^{-1}). For the computation of the saturation pressure of water over a flat surface, we follow expressions in pages 197-200 from [6] for ice and water below 30°C and Buck's equation [16] above 30°C. The dew-point temperature is given by the approximate expression 5.68 in [6] from given P and mixing ratio w.

Moist specific heats at constant pressure and volume are computed as $c_{pm} = c_{pd}(1 + 0.87q)$ and $c_{vm} = c_{vd}(1 + 0.97q)$ following [14], with $c_{pd} = 1005$ J kg^{-1}

6

K^{-1} and $c_{vd} = 718$ J kg^{-1} K^{-1} [6, 7]. By default, the functions that provide these specific heats will return the values corresponding to moist air. Values corresponding to dry air can be requested explicitly building a dry air parcel.

A good analytical expression for the latent heat of evaporation of water does not exist and an approximate expression is used. For liquid water ($T \in [233.15, 313.15]$ K interval), we use a cubic polynomial expansion based on tabulated values [15] with an absolute residual smaller than 1 J kg^{-1} and all the terms statistically significant to a 99% confidence level. By doing so, we assume that, up to the Schaefer point (about -40°C), super-cooled water can exist. For ice, the result is based on a quadratic fit to observed values [17] in the interval $T \in [210, 273.15]$ K (residuals smaller than 0.05 J kg^{-1}). Since the values corresponding to water and ice are not the same in the common interval used in the previous two expressions, a linear combination of ice's (L_i) and water's (L_w) latent heat is computed $L = w_i L_i + (1 - w_i)L_w$ with weight $w_i = 1 - \frac{T-253.15}{20}$ in the interval $T \in [253.15, 273.15]$ K. Below 253.15 K, the latent heat corresponding to ice is applied, and the latent heat corresponding to water is used above 273.15 K.

All the vertical evolutions are computed assuming hydrostatic balance. Thus, $\Gamma_d^* = \left(\frac{dT}{dP}\right)_d = \frac{\Gamma_d}{\rho g}$ and $\Gamma_s^* = \frac{\Gamma_s}{\rho g}$ are used, with Γ_d and Γ_s the usual expression for vertical gradients in Z. For the saturated pseudoadiabatic profile, the expression used in pressure coordinates is transformed from the common one in z [6, 7, 8, 14]. Using the expressions of Γ_d^* (Γ_s^*) for dry (saturated) adiabatic evolutions, the vertical evolution of an air parcel from the initial state P_0, T_0 and w_0 is computed by numerically solving the ordinary differential equation $\frac{dT}{dP} = \Gamma_i^*(P, T, w)$, with $i = d$ or $i = s$ depending whether the particle is saturated or not. This differential equation is numerically solved using a Runge-Kutta scheme of fourth order for all the vertical evolutions, with saturation checks at every vertical step.

For some of the indices (Lifted Index or Convective Available Potential Energy), it is customary to calculate a vertical average of the lower levels in order to identify a representative parcel P_0, T_0, w_0 of the lowest levels of the atmosphere [18, 19]. These vertical averages at low levels are in all cases evaluated by considering first

$$\Delta Z = \frac{R_d}{g} \int_{P_t}^{P_s} \frac{T_v dP}{P} \tag{1}$$

as the vertical width of the parcel. Next, the accumulated value of the quantity $X(P)$ in the vertical is given by the generic expression

$$\bar{X} = \frac{1}{\Delta Z} \frac{R_d}{g} \int_{P_t}^{P_s} \frac{XkT_v}{P} dP \tag{2}$$

where $k(P)$ plays the role of a normalizing function. When calculating the average temperature $k(P) = 1$ is used. Conversely, for moisture, $k(P) = q(P)$ specific humidity is used. The vertical integrals are in all cases computed using discrete slabs defined by the data given by the soundings. For these discrete slabs, the integrals are computed analytically and theese results are accumulated.

For the computation of Convective Available Potential Energy (CAPE) and Convective Inhibition (CIN), the vertical integrals are computed in pressure levels by adding the energy corresponding to discrete slabs defined by linear or

logarithmic vertical profiles defined by the soundings. The integrals for each of the slabs enclosed by linear profiles are computed analytically and the energy corresponding to each slab is accumulated to the final value of CAPE or CIN. The integrals are always performed using virtual temperature [20].

There are different ways to accurately find the Lifting Condensation Level (LCL) or the equivalent potential temperature of an air parcel in *aiRthermo*. In the first case, the library calculates these variables by computing their vertical evolutions numerically solving the ordinary differential equation representing their ascent from the initial conditions given by their temperature, pressure and mixing ratio. For compatibility, functions that allow to compute these variables from well-known alternative equations such as the approximate method by Bolton [21] to compute LCL are also provided.

A routine designed to produce Stüve diagrams either for soundings or even for the lifted particles used in the computation of CAPE/CIN extends the available options for thermodynamic diagrams in R existing in package RadioSonde. The routine that plots the Stüve diagram uses equivalent potential temperature lines, constant mixing ratio lines or dry adiabatic lines produced by the routines in *aiRthermo* for full consistency of results. The routine that plots the Stüve diagram allows the user to plot additional lines in the sounding enabling the production of very customizable plots.

4. Description of the package

The package is made of more than 40 functions, but they can be separated into six big groups according to their utility. A brief description of each set of functions is presented here, but for a full description of the functions and the parameters needed in order to run them, the manual of the package must be checked. It can be found in the web-page corresponding to the package *aiRthermo* in the Comprehensive R Archive Network (CRAN).

- **Density of dry/moist air and virtual temperature**

  The density of air can be calculated directly with the corresponding function (`densityMoist`), or by means of intermediate functions for the calculation of the density of dry air and the density of water vapour independently (`densityDry` and `densityH2Ov`). The virtual temperature of an air parcel can also be calculated directly making use of the function `virtual_temperature`.

- **Conversion of moisture indices**

  Several functions that allow the conversion between moisture indices as dew point temperature, mixing ratio and specific or relative humidity are included in *aiRthermo*. Amongst others, the most important functions of this category are those converting from relative humidity to mixing ratio (`rh2w`), from relative humidity to specific humidity (`rh2shum`), from mixing ratio to dew point temperature (`w2Td`) and from mixing ratio to specific humidity or reverse (`w2q` and `q2w`) or `e2w` for conversion from partial pressure of water vapour to mixing ratio.

- **Saturation mixing ratios or pressures**

8

In this class are included all the functions that use the Clausius-Clapeyron equation to calculate saturation mixing ratios or pressures. The most important function is `saturation_pressure_H2O` which computes the saturation pressure e_s in Pa as a function of temperature. Besides it, `saturation_mixing_ratio` returns saturation mixing ratio w_s in kg kg^{-1}.

- **State and evolution of an air parcel**

  The package calculates the internal state of a parcel from given pressure, temperature and mixing ratio with the function `parcelState`. However, to calculate the vertical evolution of an air parcel, *aiRthermo* determines which is the right function depending on the state of the particle and the environment. A general ascent from a given initial pressure to the final one is computed by the function `adiabatic_ascent`. It selects the type of evolution depending on the saturation of the parcel. A downwards evolution can also be computed with `AnyAdiabaticDown`, but it needs the initial amount of water available in the cloud for evaporation (in kg/kg). Conversions between potential temperature, temperature and pressure can be calculated making use of `PT2Theta`, `PTheta2T` and `TTheta2P`. These functions are useful if dry adiabatic processes are taking place.

- **Instability indices**

  Several functions compute common instability indices such as K, the Total-Totals, the Showalter and the Lifted index (functions `Kindex`, `TTindex`, `Sindex` and `LIindex`). `CAPE_CIN` calculates the values of CAPE and CIN, the LCL, the Level of Free Convection (LFC), the End Level (EL) and the trajectory followed by the lifted parcel. *PlowTop* argument provides the width of a slab across which a vertical average through the bottom of the sounding will be performed to get initial conditions of the ascending parcel. *precoolType* determines which type of precooling must be applied to the initial parcel. *upToTop* controls whether the lifted particle continues upwards after the first time it crosses the ambient sounding.

- **Stüve diagrams**

  The `stuve_diagram` function is included to allow the creation of high-quality Stüve diagrams. Besides the Stüve diagram, they can also represent the trajectory followed by any ascending air parcel (`CAPE_CIN` called using *getLiftedBack=TRUE*).

Figure 2 shows the Stüve diagram corresponding to the Davenport sample sounding. Major differences in the estimation of CAPE for the sounding can appear if the *upToTop* attribute is set to *TRUE* or *FALSE* (red and blue lines of the Figure) due to the lifting particle slightly crossing the sounding at low levels. These results can be controlled by using appropriate parameters. Sensible default parameters are used by the function if they are not explicitly provided by the user.

Listing 1 shows the way `CAPE_CIN` was used to produce Figure 2. The second and third times `CAPE_CIN` is called, `getLiftedBack` is set to `TRUE`, so that the trajectory of the lifted parcel is returned to the calling environment. Figure 2 shows in blue the trajectory of the ascending parcel as recorded in `capeOut2` object (`upToTop=FALSE`). It stops the first time that the ascending parcel is not
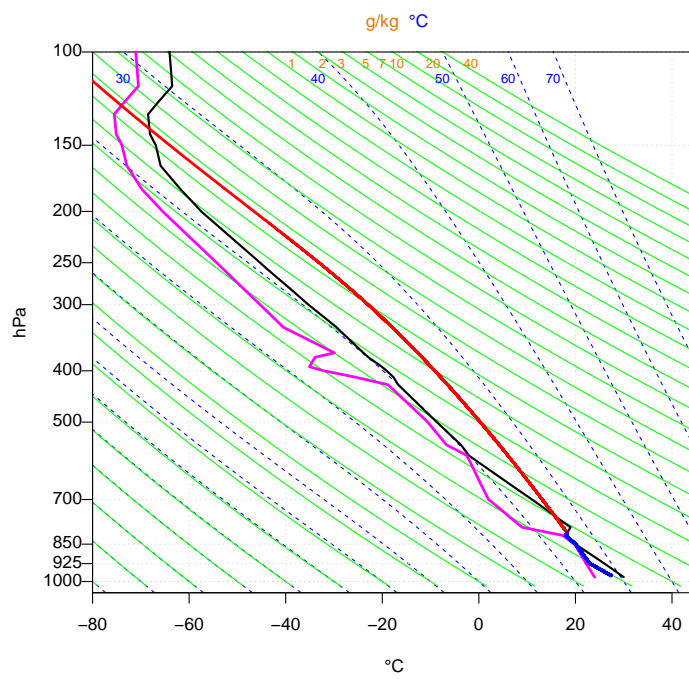
Figure 2: Example of a Stüve diagram plotted with *aiRthermo*. The temperature (black) and dew point temperature (magenta) of the sounding are plotted together with the evolution of the lifted air parcel until the moment when it crosses for the first time the ambient sounding (blue) or up to the top of the sounding (red).

buoyant, leading to a severe understimation of the value of CAPE. The red line in Figure 2 shows the evolution of the parcel stored in `capeOut` (argument `upToTop=TRUE`).

Listing 1: Evaluation of CAPE (CIN) and representation of a sounding

```
data(RadiosondeDavenport)
dPs<-RadiosondeDavenport[,1]*100
dTs<-C2K(RadiosondeDavenport[,3])
dws<-RadiosondeDavenport[,6]/1000
# Leave in Celsius for plotting
dTd<-RadiosondeDavenport[,4]

# Initial conditions are known.
# upToTop<-FALSE "stop after parcel not buoyant"
capeOut<-CAPE_CIN(Ps=dPs,Ts=dTs,ws=dws,deltaP=1,
        P0=97500,T0=300.6,w0=0.01936,
        PlowTop=NA,upToTop=FALSE,
        getLiftedBack=FALSE,precoolType="none")
# some of the info from the output object
print(paste("Davenport_CAPE:",capeOut$cape,
      "J/kg","CIN:",capeOut$cin,"J/kg","LFC",
      capeOut$apLFC$P,"Pa",capeOut$apLFC$Temp,"K",
      "EqLevel:",capeOut$apEL$P,"Pa",
      capeOut$apEL$Temp,"K"))
# Whole sounding now (upToTop<-TRUE), get parcel back
capeOut<-CAPE_CIN(Ps=dPs,Ts=dTs,ws=dws,deltaP=1,
      P0=97500,T0=300.6,w0=0.01936,PlowTop=NA,
      upToTop=TRUE,getLiftedBack=TRUE,
      precoolType="none")
capeOut2<-CAPE_CIN(Ps=dPs,Ts=dTs,ws=dws,deltaP=1,
      P0=97500,T0=300.6,w0=0.01936,
      PlowTop=NA,upToTop=FALSE,
      getLiftedBack=TRUE,precoolType="none")

pdf("stuve-with-parcel.pdf")
# Plot sounding
plot<-stuve_diagram(Pres=dPs/100,Temp=K2C(dTs))
# Dew point temperature
lines(dTd,dPs/100,col="magenta",lwd=2)
# Lifted parcel (upToTop=TRUE) in red
lines(K2C(capeOut$Tl),(capeOut$Pl/100),
      col="red",lwd=2)
# upToTop=FALSE in blue
lines(K2C(capeOut2$Tl),capeOut2$Pl/100,
      col="blue",lwd=2)
dev.off()
```

A profiler has been used to evaluate the CPU time required by *aiRthermo* to calculate a saturated adiabatic evolution from an initial level of 950 hPa to 200 hPa (pressure step of 1 Pa). A routine that performs the same computation us-
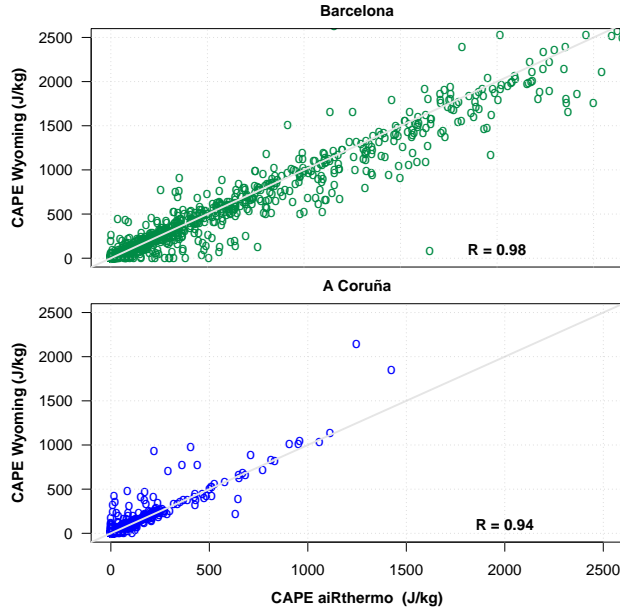
Figure 3: Scatterplot of CAPE values as computed by *aiRthermo* and the corresponding values as computed by University of Wyoming for Barcelona (top) and A Coruña (bottom).

ing an R iteration was also written. The evolution takes 50 ms with *aiRthermo*. For the pure R case, it takes around 1500 ms. Thus, there is an increase of speed of about thirty times due to the use of the C core for the computation of vertical evolutions.

5. Case study: Instability indices over the Iberian Peninsula (2010-2014)

The performance of the package has been checked with a high number of real soundings over the Iberian Peninsula (Figure 1), an area well known for the development of convective systems [22]. The results of CAPE as computed by *aiRthermo* and the value stored at the University of Wyoming server have been compared. Figure 3 shows the resulting scatterplots for A Coruña (Atlantic site) and Barcelona (Mediterranean). The value of Pearson's correlation coefficient R is very good in both cases, 0.94 in A Coruña (3521 soundings) and 0.98 in Barcelona (3575 soundings). The values of R are found in the range $[0.94, 0.99]$ in all stations.

In this case-study, 24072 soundings were processed for the eight stations. CAPE and CIN were computed using a very low vertical step (0.5 Pa) and all of them extended up to the top of the sounding. CAPE and CIN were computed twice for two different initial parcels (one from the lowest point of the sounding and the second one from a low-level average). The K, Total-Totals, Lifted and Showalter indices were also computed. This processing took six hours in a common desktop computer (2015) running Linux.

12

6. Discussion and Conclusions

This paper presents a new package for R, *aiRthermo*, that is available in the open-source repository for R packages CRAN. It provides new functions to R in the field of atmospheric thermodynamics. These capabilities considerably extend the analyses that can be performed from inside the R interpreter.

In the field of storm forecasting, the quantities that can be computed using *aiRthermo* have been used to produce storm forecasts in Belgrado [23]. Thus, the ability to run different statistical models and verification procedures from inside R together with the computation of the indices themselves could boost this kind of studies. A similar analysis [24] was carried out in the Arctic region (Bjørnøya, Jan Mayen and Svalbard Islands) with results on the distribution of instability indices very different to other regions of Europe [25]. The instability available in *aiRthermo* have been combined with satellite data in a Regional Instability Index in Africa [26] or India [27]. These results show that the analysis of the climatological distribution of atmospheric instability [25], its interannual variability and its expected future distribution [22] under global change conditions can benefit from *aiRthermo*. The fact that some of the instability indices must be computed from vertical adiabatic evolutions of air parcels close to the surface (the case of CAPE or Lifted Index) makes the analysis of these distributions easier if every sounding can be processed in a much shorter time (as performed by *aiRthermo*). This will increase the use of instability indices in downscaling methods designed to operate on daily precipitation [28] even for long periods of time.

Besides the case of precipitation forecasts, other damaging effects can derive from atmospheric convective instability. Atmospheric instability indices are used to analyze lightning in Western Patagonia [29] or the Iberian Peninsula [30]. They are also prognostic variables in exercises of statistical downscaling of wind variability [31]. The field of aircraft safety is another area where the thermodynamical properties of air, particularly when it is close to saturation, can be important, both at the surface, during the prevention of fog, such as in the study of ice fog [32] or aloft, in order to prevent aircraft icing conditions [33].

There is a perpetual need of verification of complex forecasting systems based on advanced numerical models. In these verifications, the diagnostics available in *aiRthermo* are often used [34]. The direct availability of these diagnostics from the package used for the verification (frequently R itself) will hopefully lead to a faster development of these models. This includes also new satellite systems such as GOES-R [35, 36]. It has the ability to produce almost on real time integrated instability indices such as LI. The ability to easily compute the value of LI, CAPE or other indices from soundings, satellite sounders [37, 38] and numerical model results will ease the interoperability of model and observational data (soundings, satellite-derived products and remotely sensed information) in new operational environmental forecasting systems.

7. Acknowledgements

UPV/EHU). Upper air reports provided by the server run by University of Wyoming, Dept. of Atmospheric Science are greatly acknowledged.

8. Software and data availability

The software presented in this paper is a package prepared to work within the R data analysis suite and it was developed by the authors:

- Jon Sáenz

- Santos J. González-Rojí.

- Sheila Carreno-Madinabeitia

- Gabriel Ibarra-Berastegi

Contact address: Jon Sáenz, Dept. of Applied Physics II, Faculty of Science and Technology, UPV/EHU, Barrio Sarriena s/n, 48940-Leioa, Spain.
Telephone: +34 946012445
Fax: +34 946013500
email addresses:

- jon.saenz@ehu.eus

- santosjose.gonzalez@ehu.eus

- sheila.carreno@tecnalia.com

- gabriel.ibarra@ehu.eus

Year first available in CRAN: 2017.
Hardware required: It has been tested in laptops, desktops and workstations running Mac OS, Windows and Linux.
Availability: The software and the datasets are freely available (GPL-3 license) in the Comprehensive R Archive Network (CRAN):
`https://cran.r-project.org/package=aiRthermo`
It can be installed from any of the mirrors as usually done with R packages by just typing `install.packages("aiRthermo")` inside the R interpreter. The size of the package ranges from 400 Kb to 500 Kb, depending whether the source version or the Windows compiled version is downloaded. The CRAN servers allow anonymous access to the package. The software is written either in R and C. The manual is also provided at the CRAN server [39].

[1] D. C. Carslaw, K. Ropkins, openair An R package for air quality data analysis, Environmental Modelling & Software 27-28 (2012) 52–61. `doi: 10.1016/j.envsoft.2011.09.008`.

[2] R. Serrano-Notivoli, M. de Luis, S. Beguería, An R package for daily precipitation climate series reconstruction, Environmental Modelling & Software 89 (2017) 190–195. `doi:10.1016/j.envsoft.2016.11.005`.

[3] J. Skøien, G. Blöschl, G. Laaha, E. Pebesma, J. Parajka, A. Viglione, rtop: An R package for interpolation of data with a variable spatial support, with an example from river networks, Computers & Geosciences 67 (2014) 180 – 190. `doi:10.1016/j.cageo.2014.02.009`.

[4] L. Busetto, L. Ranghetti, MODIStsp: An R package for automatic prepro-cessing of MODIS Land Products time series, Computers & Geosciences 97 (2016) 40 − 48. `doi:10.1016/j.cageo.2016.08.020`.

[5] D. Bowman, J. Lees, Near real time weather and ocean model data access with rNOMADS, Computers & Geosciences 78 (2015) 88 − 95. `doi:10.1016/j.cageo.2015.02.013`.

[6] C. F. Bohren, B. A. Albrecht, Atmospheric Thermodynamics, Oxford University Press, New York, 1998.

[7] G. W. Petty, A First Course in Atmospheric Thermodynamics, Sundog Publishing, Madison, 2008.

[8] G. R. North, T. L. Erukhimova, Atmospheric Thermodynamics, Cambridge University Press, New York, 2009.

[9] Z. Liang, D. Wang, Sea breeze and precipitation over Hainan Island, Quarterly Journal of the Royal Meteorological Society 143 (2017) 137–151. `doi:10.1002/qj.2952`.

[10] C. A. Doswell III, H. E. Brooks, R. A. Maddox, Flash flood forecasting: An ingredients-based methodology, Weather and Forecasting 11 (1996) 560–581. `doi:10.1175/1520-0434(1996)011<0560:FFFAIB>2.0.CO;2`.

[11] V. Petković, C. D. Kummerow, Understanding the sources of satellite passive microwave rainfall retrieval systematic errors over land, Journal of Applied Meteorology and Climatology 56 (2017) 597–614. `doi:10.1175/JAMC-D-16-0174.1`.

[12] G. Ibarra-Berastegi, J. Sáenz, A. Ezcurra, A. Elías, J. Díaz de Argandoña, I. Errasti, Downscaling of surface moisture flux and precipitation in the Ebro Valley (Spain) using analogues and analogues followed by random forests and multiple linear regression, Hydrology and Earth System Sciences 15 (2011) 1895–1907. `doi:10.5194/hess-15-1895-2011`.

[13] J. Sáenz, S. González-Rojí, S. Carreno-Madinabeitia, G. Ibarra-Berastegi, Airthermo: An R package designed to help students understanding atmospheric thermodynamics, in: EDULEARN18 Proceedings, 10th International Conference on Education and New Learning Technologies, IATED, 2018, pp. 1567–1573.

[14] A. A. Tsonis, An Introduction to Atmospheric Thermodynamics, Cambridge University Press, Cambridge, 2002.

[15] R. R. Rogers, M. K. Yau, A Short Course in Cloud Physics, 3rd Edition, Pergamon Press, Oxford, 1989.

[16] A. L. Buck, New equations for computing vapor pressure and enhancement factor, Journal of Applied Meteorology 20 (1981) 1527–1532. `doi:10.1175/1520-0450(1981)020<1527:NEFCVP>2.0.CO;2`.

[17] R. Feistel, W. Wagner, A new equation of state for H2O ice Ih, Journal of Physical and Chemical Reference Data 35 (2006) 1021–1047. `doi:10.1063/1.2183324`.

[18] J. P. Craven, R. E. Jewell, H. E. Brooks, Comparison between observed convective cloud-base heights and lifting condensation level for two different lifted parcels, Weather and Forecasting 17 (2002) 885–890. `doi:10.1175/1520-0434(2002)017<0885:CBOCCB>2.0.CO;2`.

[19] C. E. Letkewicz, M. D. Parker, Forecasting the maintenance of mesoscale convective systems crossing the Appalachian Mountains, Weather and Forecasting 25 (2010) 1179–1195. `doi:10.1175/2010WAF2222379.1`.

[20] C. A. Doswell III, E. N. Rasmussen, The effect of neglecting the virtual temperature correction on CAPE calculations, Weather and Forecasting 9 (1994) 625–629. `doi:10.1175/1520-0434(1994)009<0625:TEONTV>2.0.CO;2`.

[21] D. Bolton, The computation of equivalent potential temperature, Monthly Weather Review 108 (1980) 1046–1053. `doi:10.1175/1520-0493(1980)108<1046:TCOEPT>2.0.CO;2`.

[22] C. Viceto, M. Marta-Almeida, A. Rocha, Future climate change of stability indices for the Iberian Peninsula, International Journal of Climatology n/a (2017) 4390–4408. `doi:10.1002/joc.5094`.

[23] D. Vujović, M. Paskota, N. Todorović, V. Vučković, Evaluation of the stability indices for the thunderstorm forecasting in the region of belgrade, serbia, Atmospheric Research 161 (2015) 143 – 152. `doi:10.1016/j.atmosres.2015.04.005`.

[24] B. Czernecki, M. Taszarek, L. Kolendowicz, K. Szyga-Pluta, Atmospheric conditions of thunderstorms in the European part of the Arctic derived from sounding and reanalysis data, Atmospheric Research 154 (2015) 60 – 72. `doi:10.1016/j.atmosres.2014.11.001`.

[25] M. Siedlecki, Selected instability indices in Europe, Theoretical and Applied Climatology 96 (2009) 85–94. `doi:10.1007/s00704-008-0034-4`.

[26] E. de Coning, M. Koenig, J. Olivier, The combined instability index: a new very-short range convection forecasting technique for southern Africa, Meteorological Applications 18 (2011) 421–439. `doi:10.1002/met.234`.

[27] S. Chaudhuri, J. Pal, A. Middey, S. Goswami, Nowcasting Bordoichila with a composite stability index, Natural Hazards 66 (2013) 591–607. `doi:10.1007/s11069-012-0504-y`.

[28] T. Iizumi, M. Nishimori, K. Dairaku, S. A. Adachi, M. Yokozawa, Evaluation and intercomparison of downscaled daily precipitation indices over Japan in present-day climate: Strengths and weaknesses of dynamical and bias correction-type statistical downscaling methods, Journal of Geophysical Research: Atmospheres 116 (D1) (2011) D01111. `doi:10.1029/2010JD014513`.

[29] R. D. Garreaud, M. G. Nicora, R. E. Bürgesser, E. E. Ávila, Lightning in Western Patagonia, Journal of Geophysical Research: Atmospheres 119 (2014) 4471–4485. `doi:10.1002/2013JD021160`.

[30] J. A. Santos, M. A. Reis, F. De Pablo, L. Rivas-Soriano, S. M. Leite, Forcing factors of cloud-to-ground lightning over Iberia: regional-scale assessments, Natural Hazards and Earth System Sciences 13 (7) (2013) 1745–1758. `doi:10.5194/nhess-13-1745-2013`.

[31] R. J. Davy, M. J. Woods, C. J. Russell, P. A. Coppin, Statistical downscaling of wind variability from meteorological fields, Boundary-Layer Meteorology 135 (2010) 161–175. `doi:10.1007/s10546-009-9462-7`.

[32] I. Gultepe, B. Zhou, J. Milbrandt, A. Bott, Y. Li, A. Heymsfield, B. Ferrier, R. Ware, M. Pavolonis, T. Kuhn, J. Gurka, P. Liu, J. Cermak, A review on ice fog measurements and modeling, Atmospheric Research 151 (2015) 2 – 19. `doi:10.1016/j.atmosres.2014.04.014`.

[33] B. C. Bernstein, C. A. Wolff, F. McDonough, An inferred climatology of icing conditions aloft, including supercooled large drops. Part I: Canada and the continental United States, Journal of Applied Meteorology and Climatology 46 (2007) 1857–1878. `doi:10.1175/2007JAMC1607.1`.

[34] T. A. Jones, S. Koch, Z. Li, Assimilating synthetic hyperspectral sounder temperature and humidity retrievals to improve severe weather forecasts, Atmospheric Research 186 (2017) 9 – 25. `doi:10.1016/j.atmosres.2016.11.004`.

[35] T. J. Schmit, J. Li, J. Li, W. F. Feltz, J. J. Gurka, M. D. Goldberg, K. J. Schrab, The GOES-R advanced baseline imager and the continuation of current sounder products, Journal of Applied Meteorology and Climatology 47 (2008) 2696–2711. `doi:10.1175/2008JAMC1858.1`.

[36] T. J. Schmit, J. Li, S. A. Ackerman, J. J. Gurka, High-spectral- and high-temporal-resolution infrared measurements from geostationary orbit, Journal of Atmospheric and Oceanic Technology 26 (2009) 2273–2292. `doi:10.1175/2009JTECHA1248.1`.

[37] S. J. Lee, M.-H. Ahn, Y. Lee, Application of an artificial neural network for a direct estimation of atmospheric instability from a next-generation imager, Advances in Atmospheric Sciences 33 (2016) 221–232. `doi:10.1007/s00376-015-5084-9`.

[38] T. J. Schmit, P. Griffith, M. M. Gunshor, J. M. Daniels, S. J. Goodman, W. J. Lebair, A closer look at the ABI on the GOES-R series, Bulletin of the American Meteorological Society 98 (2017) 681–698. `doi:10.1175/BAMS-D-15-00230.1`.

[39] J. Sáenz, S. J. González-Rojí, S. Carreno-Madinabeitia, G. Ibarra-Berastegi, aiRthermo: Atmospheric Thermodynamics and Visualization, r package version 1.2 (2018).
URL `https://CRAN.R-project.org/package=aiRthermo`